Balanced SSFP profile asymmetries detect small frequency shifts in white matter

K. L. MILLER[1], AND P. JEZZARD[1]

[1]FMRIB CENTRE, OXFORD UNIVERSITY, OXFORD, OXON, UNITED KINGDOM

INTRODUCTION. The balanced SSFP signal is sensitive to resonance frequency (f_0), typically described as a symmetric dependence with respect to the experimental center frequency [1]. However, we recently observed that the signal measured in white matter is strongly asymmetric [2]. Based on known effects of lineshape on SSFP signal [3], we suggest that these asymmetries reflect multiple, frequency-shifted pools, and therefore may be a marker of tissue microstructure. As a first step to elucidating the pools contributing to thse asymmetries, we fit a simple signal model to a range of measurements.

THEORY. The standard model for the SSFP signal assumes homogeneous f_0, T_1 and T_2 [1]. The resulting profile is symmetric with respect to frequency (Fig. 1 a-c, gray). The profile repeats to form "bands" every T_R^{-1} Hz and the signal phase in adjacent bands differs by 180°. In a voxel containing multiple frequencies (i.e., a lineshape), the signal profile is the convolution of this predicted profile with the lineshape [3, 4]. For an asymmetric lineshape (Fig. 1d), this results in an asymmetric SSFP profile (Fig. 1a-c, blue and green). The 180° phase shift between adjacent bands can create phase cancellation between parts of the lineshape at relatively small frequency offsets (Fig. 1a-d, green). Thus, the asymmetries may be sensitive to minute details of the lineshape. However, because the profile repeats, large frequency shifts can occupy neighboring bands (Fig. 1a-d, blue), and effectively alias to create the same effect. The size of shift is highly relevant to the source of asymmetries (for example, fat shifts ~100 Hz, while most water shifts are smaller).

METHODS. Balanced SSFP images were acquired in 8 subjects and one post-mortem brain. After each volume acquisition, the frequency was shifted, and acquisition was repeated at enough frequencies to cover the SSFP profile (profile width=T_R^{-1}, at 1 Hz resolution). Other parameters see [2]. We implemented a simple model that convolves a lineshape function with the calculated SSFP profile. Our modeled lineshape is a sum of two shifted Lorentzians, described by 4 parameters: widths Γ_1 and Γ_2, volume fraction v and frequency shift Δf. We also fit SSFP parameters about which there is some uncertainty: T_1:T_2 ratio, α, f_0 and an arbitrary scale factor, which converged to reasonable values for all fits presented. Non-linear fitting was performed in Matlab with multiple starts (n_{start}=300) to avoid local minima. Initial fits used broad bounds on lineshape parameters (-500<Δf<500 Hz; 0<Γ_1, Γ_2<20 Hz), and subsequent fits tightened these bounds once large shifts could be ruled out (-40<Δf<40 Hz; 0<Γ_1<20 Hz, Γ_2=0.1).

MULTI-T_R DATA. The profile dependence on T_R reflects the size of shifts: pools with large frequency shifts have a strong dependence on T_R, but small shifts do not (Fig. 1a-d). For one in vivo (Fig. 1e-g) and one post-mortem (Fig. 1h-j) experiment at T_R=10-20 ms, profiles were extracted from the corpus callosum. The measured shapes exhibit subtle variations with changing T_R, which is the predicted behavior for small frequency shifts. This observation is validated by fits (simultaneous to data at T_R=10-20 ms), which converged to small frequency shifts despite broad search bounds (fitted params in Fig. 1).

MULTI-SUBJECT DATA. Comparing voxel-wise maps of the SSFP asymmetry index (high AI = strong asymmetry) to DTI data demonstrates that the amount of asymmetry correlates to tract direction, with reduced AI in tracts running parallel to B_0 (Fig. 2a-c, and another abstract by our group). This directional dependence may be an important clue for understanding the source of asymmetries. Using white matter masks corresponding to tract centers (generated using TBSS [5], Fig. 2b), we generated two ROIs for each subject corresponding to tracts that are parallel (D_z>D_{xy}) and perpendicular (D_{xy}>2D_z) to B_0. The mean profiles for each ROI in each subject were fit separately, and the fits to these different types of tracts are given in Table 1. The frequency offset (Δf) and width (Γ_1) consistently differ between tract types, with both parameters increasing for the more asymmetric orthogonal tracts.

DISCUSSION. SSFP profile asymmetries in white matter cannot be caused by T_1, T_2 or diffusion, but can be explained by lineshape effects at small frequency shifts. This creates a novel contrast mechanism that may be sensitive to tissue microstructrue properties that affect white matter lineshape. Based on model fits, the small (v=15-20%), broad component may correspond to short T_2 species [6], or to effects related to tract geometry [7].

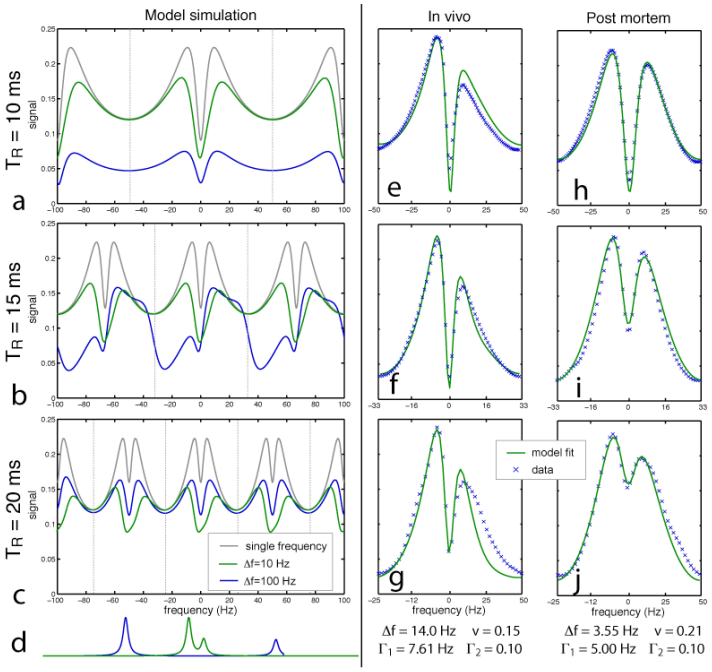

FIGURE 1: (d) Lineshapes with large (blue) and small (green) frequency shifts. (a-c) The SSFP profile for large shifts varies strongly with T_R, unlike small shifts, due to aliasing of the large shifts into adjacent bands (vertical lines). (e-j) Data at multiple T_R (blue x) do not exhibit profound shape changes, indicating small shifts, in good agreement with model fits (green).

	Δf (Hz)	v	Γ_1 (Hz)	Γ_2 (Hz)
Parallel to B_0	6.1 ± 2.5	0.28 ± 0.15	6.0 ± 3.9	Fixed 0.1
Orthogonal to B_0	15.1 ± 3.8	0.19 ± 0.05	8.7 ± 1.4	Fixed 0.1

TABLE 1: Fitted lineshape parameters across 6 subjects (mean ± stdev).

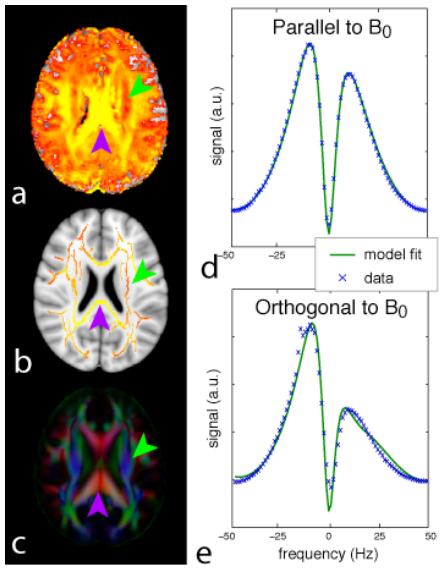

FIGURE 2: (a) Subject asymmetry index (AI) map. (b) AI projected onto subject-specific white matter skeleton. (c) DTI tract direction map (x=red, y=green, z=blue). AI is low in tracts parallel to B_0 (green arrow) and high in tracts orthogonal to B_0 (purple arrow). ROIs based on tract direction in DTI data are used to calculate SSFP profiles for tracts (d) parallel and (e) orthogonal to B_0. These profiles are fit separately for each subject, and the fit parameters relating to the lineshape reflect the differences in asymmetry (Table 1).

[1] Oppelt, Electromed 1986.
[2] Miller, ISMRM 2008.
[3] Scheffler, NMR Biomed 2001.
[4] Miller, MRM 2008.
[5] Smith, NeuroImage 2006.
[6] Mackay, MRI 2006.
[7] Yablonskiy, MRM, 1994.